La Ciega Historical building. LUZ first headquarter

REVISTA TÉCNICA
DE LA FACULTAD DE INGENIERÍA

An international refereed Journal indexed by:

- SCOPUS
- SCIELO
- LATINDEX
- DOAJ
- MIAR
- REDIB
- AEROSPACE DATABASE
- CIVIL ENGINEERING ABTRACTS
- METADEX
- COMMUNICATION ABSTRACTS
- ZENTRALBLATT MATH, ZBMATH
- ACTUALIDAD IBEROAMERICANA
- BIBLAT
- PERIODICA
- REVENCYT

"Post nubila phoebus"

"After the clouds, the sun"

LUZ in its 130th anniversary
Established since 1891

REVISTA TÉCNICA
DE LA FACULTAD DE INGENIERÍA

UNIVERSIDAD DEL ZULIA

| VOLUME 44 | MAY - AUGUST 2021 | NUMBER 2 |

Experimental Behavior of Welded Connections between Square Steel Tubes Formed by G profiles of 60x30x10x2 and 80x40x15x3 mm Subject to Monotonic Loads

Carlos Alberto Romero Romero[1*] ⓘ *, Franklin Paul Verdugo Astudillo*[1] ⓘ *, Julio Sebastián Bejarano Saritama*[1] ⓘ *, José Domingo Alviar Malabet*[1] ⓘ *, y Nelson Andrés López Machado*[2] ⓘ

[1]Universidad Politécnica Salesiana, Avenida Morán Valverde y Rumichaca, PB EC170105, Quito, Ecuador
[2]Pontifica Universidad Católica, Santiago de Chile, 7560801, Chile
*Corresponding author: cromero@ups.edu.ec
https://doi.org/10.22209/rt.v44n2a04
Received: 04 July 2020 | Accepted: 05 March 2021 | Available: 15 April 2021

Abstract

In Ecuador, the use of square tubular steel connections has increased in houses and shopping centers. However, there is no regulation that explains the behavior of the connection. In this research, the experimental behavior of this connection was evaluated. For this purpose, tests were carried out where the elastoplastic behavior of welded joints with square steel tubes formed by G profiles of 60x30x10x2 and 80x40x15x3 mm, subject to monotonic loads, were analyzed. Each test consisted of imposing a progressive load on the frame upper node, in order to measure the displacements and distortion of the geometry of the beam-column join elements of the lower connection. Results show that the experimental collapse load in frames 1, 2 and 3 (connection without reinforcement) decreased 12.82 % with respect to the theoretical value, while the collapse in frames 4, 5 and 6 (reinforced connection) increased by 14.96 %. The reinforcement was constituted by platens installed in the column of the lower connection. With this, the failure due to local buckling has been avoided and the formation of plastic hinges in the beam of the welded joint has been guaranteed, thus fulfilling the criterion of weak beam-strong column.

Keywords: monotonic load, welded connection, G profiles, plastic hinge.

Comportamiento Experimental de Conexiones Soldadas entre Tubos Cuadrados de Acero Conformados por Perfiles G de 60x30x10x2 y 80x40x15x3 mm Sometidas a Carga Monotónica

Resumen

En el Ecuador se ha incrementado el uso de conexiones con tubulares cuadrados de acero en viviendas y centros comerciales. Sin embargo, no existe una normativa que explique su comportamiento. En esta investigación se evaluó el comportamiento experimental de dicha conexión. Para ello, se realizaron ensayos donde se analizó el comportamiento elastoplástico de juntas soldadas con tubos cuadrados de acero conformados por perfiles G de 60x30x10x2 y 80x40x15x3 mm, sometidas a carga monotónica. Cada prueba consistió en imponer carga progresiva en la conexión superior del pórtico, para medir los desplazamientos y distorsión de la geometría de los elementos unión viga-columna de la conexión inferior. Los resultados evidencian que la carga de colapso experimental en los pórticos 1, 2 y 3 (conexión sin refuerzo) disminuyó 12,82 % con respecto al valor teórico, mientras que en los pórticos 4, 5 y 6 (conexión reforzada) se incrementó en 14,96 %. El reforzamiento está conformado por platinas instaladas en la columna de la conexión inferior. Con ello, se ha evitado la falla por pandeo local y se ha garantizado la formación de rótulas plásticas en la viga de la unión soldada, cumpliendo así el criterio de viga débil-columna fuerte.

Palabras clave: carga monotónica, conexión soldada, perfiles G, rótula plástica**.**

Introduction

Until recently the elastic behavior of materials (Hibbeler, 2017) was used for designing structures (Kassimali, 2015), due to the little knowledge about the behavior of materials subject to deformations exceeding the elastic ones. However, important advances in models based on the theory of frames, have attempted to represent the stages of the real behavior of structures, and this is how nonlinear plastic models that consider large displacements and deformations, under static and dynamic requirements (NEC-SE-CG, 2014; NEC-SE-DS, 2014), have been developed.

As explained earlier, Ugarte *et al.* (2006) evaluated the behavior of square tubulars to bending with monotonical load, whose modeling is implemented using the software Abaqus. However, the study focuses on tubular elements without reinforcement. Carapaz (2015) studied the behavior of steel tubulars subject to axial load with the alternative of internally filling the tubular with concrete. González (2016) evaluated the behavior of bolted joints of squared tubulars cold formed without using reinforcement plates and welding as join element. Fadden (2013) studied the connection between cold formed squared tubular elements subject to monotonic and cyclic loads, the reinforcement consisted in placing a stiffening sheet that surrounds the perimeter of the column and rests on the flanges of the top and base beams using full penetration welding.

Rezaifar and Younesi (2017) carried out an analytical study of the beam-column connection with trapezoidal stiffeners welded to the flanges of type I-beams, as opposed to the case proposed in this study where plates that surround the perimeter of the square-section column are installed.

One of the constructive forms extensively used in Ecuador is joining cold-bent G profiles (Novacero, 2017) and form square-section steel tubulars through the use of fillet or full penetration welding. However, there is uncertainty in the plastic behavior of the welded beam-column connection between these elements (Pellicer, 2014).

As explained earlier, in this research it was evaluated the behavior of such connection by means of experimental tests, in order to appreciate the distortion of the cross section of the weld connected beam and column (With and without reinforcement) (Romero, 2010).

The experimental tests allow the elastic and plastic behavior analysis of the weld joint elements, which is essential to avoid possible failure mechanisms that may occur in the building (NEC-SE-AC, 2014), especially, if the node does not fulfill the strong column-weak beam criterion (ANSI/AISC, 2010).

Experimental

Determination of the collapse load in the tested frames

The collapse load of the tested frames was determined with the theory of plastic analysis (Seguí, 2013). For that a collapse mechanism is proposed (Figure 1).

Collapse mechanism in the frames.   Plastic hinge mechanism.
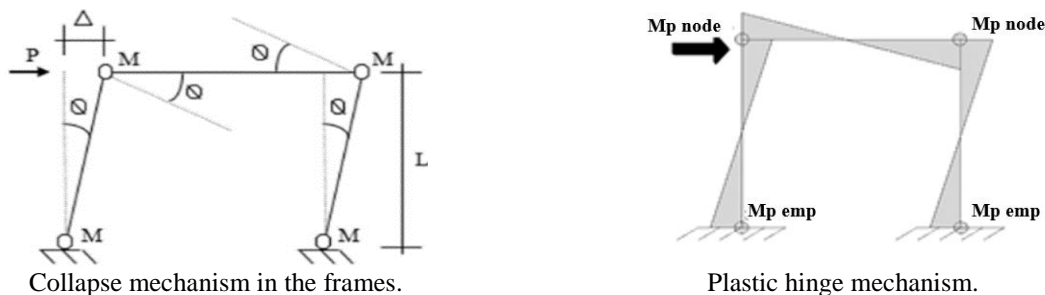
Figure 1. Plastic analysis of the frames collapse mechanism (Seguí, 2013).

The calculations were carried out using Equation 1 (Seguí, 2013).

$$W_{ext}=W_{int} \tag{1}$$

Where:

W_{ext}; is external work; W_{int} is internal work.

$$P\Delta=2\left(Mp_{emp}+Mp_{node}\right)*\theta, \text{ but } \Delta \text{ is equal to } \Delta=\theta*L, \text{ then}$$

$$P*\theta*L =2\left(Mp_{emp}+Mp_{node}\right)*\theta$$

From this Mp_{emp} is equal to Mp_{node} The calculations for the collapse load "P" were carried out using Equation 2.

$$P=\frac{4M_n}{L}=\frac{4*1.25*S_e*F_y}{L} \tag{2}$$

Where:

Mn is nominal plastic moment; Se is elastic section modulus (AISI, 1996); Fy is yield stress (Cervera, 2015); L is length of the element, set at 45 cm; 1.25 is shape factor to convert from elastic moment to plastic moment.

Substituting in Equation 2, the mechanical properties 1.25 Se, Fy and L, as shown in Table 1, the load "P" in each case resulted as:

Table 1. Collapse load in the tested frames.

Frame	Se (cm^3)	Fy (kgf/cm^2)	L (cm)	P (N)
Frame 1 beam and column 60x60x2mm square tube	9.22	2,531	45.00	25,436
Frame 2 beam and column 80x80x3mm square tube	24.52	2,531	45.00	67,646
Frame 3 beam 60x60x2mm square tube column 80x80x3mm square tube	24.52	2,531	45.00	67,646

Se: elastic section modulus, Fy: yield stress, L: length of the element, P: applied load.

Analysis and design of the nondeformable support framing

The geometry of the rigid framing for the assembly of the tested frames is shown in Figure 2.
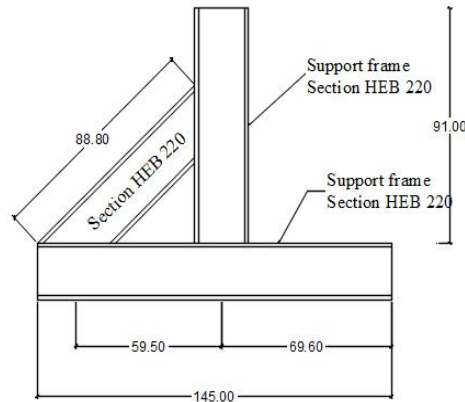
Figure 2. Geometry of the rigid framing for the assembly of the tested frames. Specifications cm.

The analysis of the framing was developed with the SAP 2000 (2017) software, while the design for bending and the shear evaluation was performed with the theory of permissible stress (McCormac, 2012). The calculations were carried out employing Equations 3 and 4 using a load in service condition of 78,453 N, i.e., approximately 1.2 times more the collapse load of 67,646 N for the most rigid frame tested, with this the shear and maximum moment resulted: 16,381.5 Kgf and 4,386.5 Kgf.m (Figure 3).

| Maximum shear in support framing. | Maximum moment in support framing. |
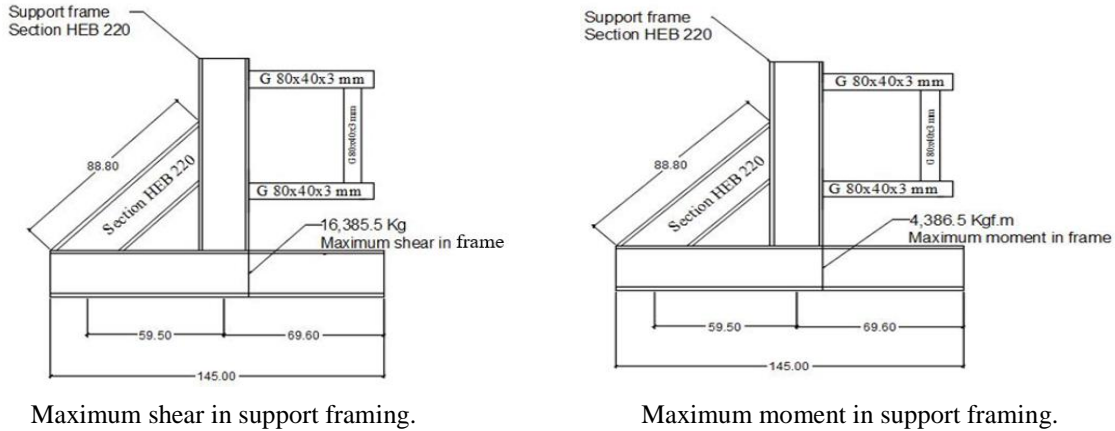
Figure 3. Analysis of the support framing in the (SAP 2000, 2017) software. Specifications cm.

$$Fb=0.60Fy\geq fb=\frac{M}{Sx} \tag{3}$$

Where:
Fb is permissible bending stress; Fy is yield stress of the steel; fb is acting bending stress; M is acting moment; Sx is elastic section modulus.

$$Fv=0.40Fy\geq fv=\frac{V}{Aw.d} \tag{4}$$

Where:
Fv is permissible shear stress; V is acting shear; Aw is the profile web thickness; d is the web height; Fy is yield stress of the steel.

Substituting the maximum moment in service condition of 438,650 kgf.cm Equation 3, the elastic section modulus Sx resulted:

$$Sx=\frac{M}{0.6*F_y}=\frac{438,650\ kgf.cm}{0.6*2,531(kgf/cm^2)}=288.85\ cm^3$$

With this result, a HEB160 profile (Novacero, 2017) was obtained. However, to prevent the failure due to shear, it was selected a HEB220 profile; with a web area of 17.86 cm2 and a yield of 2,531 kg/cm2 (ASTM, 2014), such that when substituting in Equation 4 the acting shear stress resulted:

$$fv=\frac{16,381.50\ kgf}{17.86\ cm^2}=917.2\ kgf/cm^2 \leq 1,012.42\ kgf/cm^2$$

Calculation of the reinforcement platens

In order to determine the dimensions of the reinforcement platen, the beam-column connection of square cross section constituted by G 80x80x15x3 mm profiles was considered, and the theoretical foundation that the resisting moment of the column should be 1.10 times larger than the one corresponding to the beam (NEC-SE-AC, 2014). For this purpose, it was developed an Excel sheet whose data is shown in Table 2 and results in Table 3.

Table 2. Input data of the column reinforced with a platen of 25x2 mm.

Profile data in mm/cm		
h	84	8.40
b	42	4.20
h_1	15	1.50
t	3	0.30
r	3	0.30

h: profile height, b: profile width, h1: folding length of the flange, t: thickness, r: radius of curvature.

Table 3. Nominal plastic moment results for the reinforced column.

Profile without reinforcement		Profile with reinforcement		(e) (mm)
Wx (cm³)	12.26	Wx (cm³)	13.59	2.000
Mn (Kgf.cm)	77,751	Mn (Kgf.cm)	85,984	2.000

Wx: section modulus, Mn: nominal plastic moment, e: reinforcement platen thickness.

From the results it is observed that the nominal moment of the section with reinforcement (plate with a thickness of 2 mm) is 85,984 Kgf.cm, i.e., 10.58 % larger than the one corresponding to the section without reinforcement which is 77,571 Kgf.cm.

Hence, it was obtained a plate thickness of 2 mm. However, it was selected a commercial plate (Novacero, 2017) with the thickness of the most rigid tube, i.e., 3 mm, and 25 mm width.

Tests performed.

The mechanical properties of the G profiles that were welded to form the square section of the beam-column connection of the tested frames are shown in Table 4.

Table 4. Mechanical proper ties of the cold formed G profiles (Novacero, 2017).

G profiles (mm)	Area cm²	Ix cm⁴	Iy cm⁴	Wx cm³	h/t
60x30x10x2	2.54	14.88	5.28	4.90	30
80x40x15x3	5.11	49.04	10.85	12.26	27

Ix: inertia in the x direction, Iy: inertia in the y direction, Wx: section modulus, h/t: height/thickness ratio.

The geometry of the tested frames without and with reinforcement are shown in Figures 4 and 5.
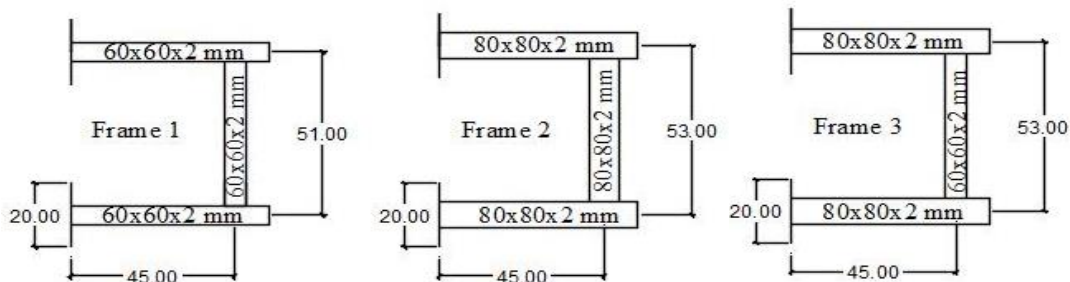
Figure 4. Geometry of the tested frames 1, 2 and 3, without reinforcement.
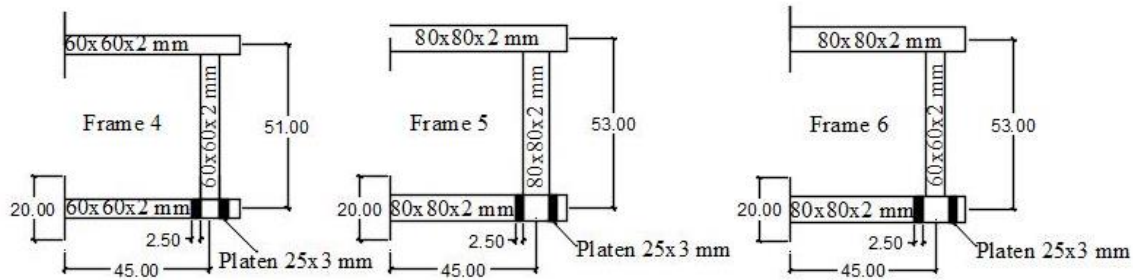
Figure 5. Geometry of the tested frames 4, 5 and 6, with reinforcement.

The set constituted by support framing and frames was placed at the of the universal testing machine (UTM). Each test consisted in imposing a progressive load at the upper joint of the frame   (Figure 6a). Subsequently, it was systematically measured the displacement of the lower joint using a measuring tape (Figure 6b). Then, to evaluate the distortion of the cross section in the elements of the lower connection, it was necessary to measure with a vernier, as shown in (Figure 6c), parameters such as: widening of the cross section of the column and beam, called (C1) and (V1), respectively.
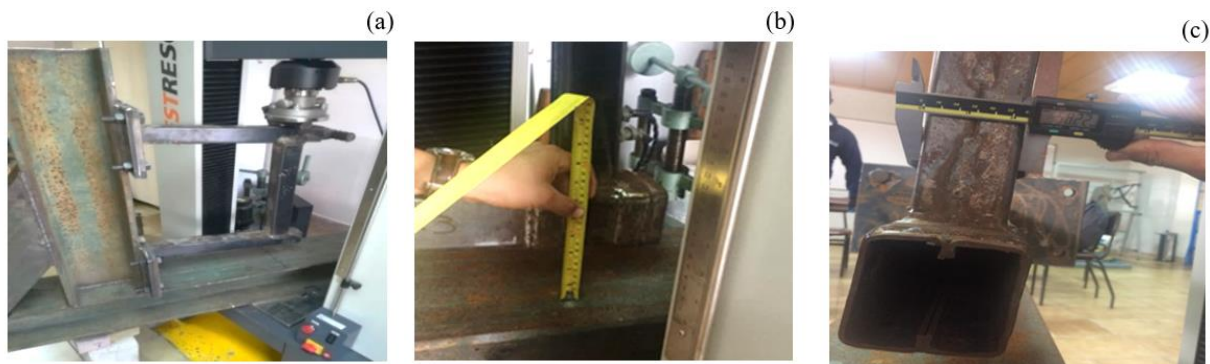
Figure 6. (a) Application of progressive load to the upper joint of the tested frames, (b) Measurement of the displacement of the lower joint of the tested frames, (c) Measurement with a vernier of the widening of the cross section of the welded joint beam, (V_1) doing the same for the columns (C_1).

Results and Discussion

Tables 5 to 10 show the results of the tests, which were used as sources for the plots shown in Figures 9 to 11; applied load vs. vertical displacement, applied load vs. widening of the cross section of the column (C_1) and applied load vs. widening of the cross section of the beam (V_1). Figure 12 represents the experimental behavior of the connection.

It may be observed in Tables 5 to 7 that the experimental collapse load in frames 1, 2 and 3 (connection without reinforcement) decreases 12.82 % (arithmetic mean) with respect to the theoretical one, which is due to a failure as a result of an excessive load that distorts the cross section of the column (local buckling), thus a plastic hinge is formed in those elements.

It may be observed in Tables 8 to 10 that the experimental collapse load in frames 4, 5 and 6 (column of the lower connection reinforced with plates) increases 14.96 % (arithmetic mean), while the displacement with respect to frames 1, 2 and 3 decreases 47.36 % (arithmetic mean). This is due to the increase of the frame lateral rigidity as a result of the addition of the reinforcement.

Table 5. Record of experimental data for frame 1, square beam and column formed with 60x30x10x2 mm G profiles.

Frame 1				
Experimental load (N)	Theoretical load (N)	Displacement (cm)	Column 60x60x2 mm Widening (C_1) (mm)	Beam 60x60x2 mm Widening (V_1) (mm)
0	25,436	0.00	0.00	0.00
4,000		0.00	0.03	0.00
8,000		0.30	0.07	0.02
12,000		0.40	0.21	0.02
16,000		0.55	0.34	0.03
20,000		0.95	6.96	0.04
19,900		2.40	10.41	0.04

Table 6. Record of experimental data for frame 2, square beam and column formed with 80x80x15x3 mm G profiles.

Frame 2				
Experimental load (N)	Theoretical load (N)	Displacement (cm)	Column 80x80x3 mm Widening (C_1) (mm)	Beam 80x80x3 mm Widening (V_1) (mm)
0	67,646	0.00	0.00	0.00
4,000		0.30	0.00	0.00
8,000		0.40	0.00	0.00
12,000		0.45	0.00	0.00
16,000		0.50	0.00	0.00
20,000		0.50	0.00	0.00
25,000		0.55	0.00	0.00
30,000		0.60	0.00	0.00
40,000		0.65	0.39	0.00
45,000		0.70	0.39	0.11
45,000		1.00	0.39	0.15
50,000		1.40	0.39	0.15
60,000		2.00	0.39	0.17
63,000		3.20	3.64	1.02
65,000		3.70	8.63	1.30
66,000		4.60	11.36	1.60
63,000		5.50	14.11	1.71

Table 7. Record of experimental data for frame 3, square beam formed with 60x30x10x2 mm G profiles and square column formed by 80x40x15x3 mm G profiles.

Experimental load (N)	Theoretical load (N)	Displacement (cm)	Column 80x80x3 mm Widening (C_1) (mm)	Beam 60x60x2 mm Widening (V_1) (mm)
Frame 3
0	67,646	0.00	0.00	0.00
4,000		0.20	0.00	0.00
8,000		0.30	0.00	0.00
12,000		0.40	0.00	0.00
16,000		0.50	0.00	0.00
20,000		0.60	0.05	0.00
25,000		0.80	0.30	0.15
30,000		0.90	0.92	0.18
35,000		1.05	0.95	0.20
40,000		1.40	1.07	0.37
45,000		1.61	2.12	0.51
50,000		2.00	2.38	0.58
55,000		2.50	3.21	0.68
60,000		3.50	4.37	0.77
61,000		3.70	5.37	0.96

Table 8. Record of experimental data for frame 4, square beam and column formed with 60x30x10x2 mm G profiles, column reinforced with 25x3 mm platens.

Experimental Load (N)	Displacement (cm)	Column 60x60x2 mm Widening (C_1) (mm)	Beam 60x60x2 mm Widening (V_1) (mm)
Frame 4
0	0.00	0.00	0.00
4,000	0.00	0.00	0.00
8,000	0.16	0.00	0.00
12,000	0.20	0.02	0.16
16,000	0.28	0.06	0.25
20,000	0.46	0.12	0.31
24,000	1.14	0.16	0.36

Table 9. Record of experimental data for frame 5, square beam and column formed with 80x40x15x3 mm G profiles, column reinforced with 25x3 mm platens.

Frame 5			
Experimental load (N)	Column (cm)	Column 80x80x3 mm Widening (C_1) (mm)	Beam 80x80x3 mm Widening (V_1) (mm)
0	0.00	0.00	0.00
4,000	0.15	0.00	0.00
8,000	0.20	0.00	0.00
12,000	0.30	0.00	0.00
16,000	0.40	0.20	0.50
20,000	0.50	0.28	0.60
25,000	0.61	0.35	0.80
35,000	0.78	0.42	0.90
45,000	1.00	0.50	1.10
50,000	1.15	0.67	1.40
55,000	1.40	0.79	1.50
60,000	1.70	0.85	1.63
65,000	2.20	0.90	1.69
69,000	3.10	0.99	1.75

Table 10. Record of experimental data for frame 6, square beam formed with 60x30x10x2 mm G profiles and square column formed by 80x40x15x3 mm G profiles, column reinforced with 25x3 mm platens.

Frame 6			
Experimental load (N)	Displacement (cm)	Column 80x80x3 mm Widening (C_1) (mm)	Beam 60x60x2 mm Widening (V_1) (mm)
0	0.00	0.00	0.00
4,000	0.10	0.00	0.00
8,000	0.15	0.00	0.08
12,000	0.22	0.00	0.15
16,000	0.29	0.00	0.21
20,000	0.35	0.00	0.24
25,000	0.41	0.17	0.30
30,000	0.52	0.23	0.38
35,000	0.60	0.28	0.46
40,000	0.70	0.35	0.52
45,000	0.77	0.40	0.58
50,000	0.88	0.47	0.67
55,000	1.01	0.56	0.79
60,000	1.15	0.68	0.88
65,000	1.40	0.87	1.10
70,000	2.00	1.60	2.01
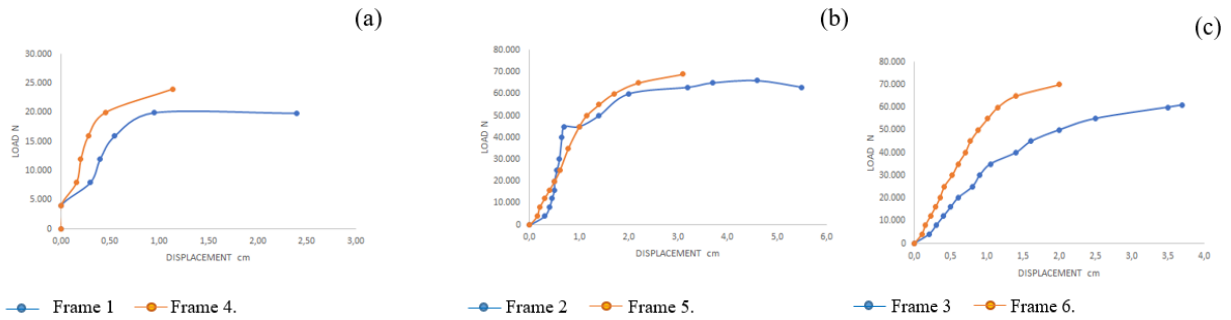
Figure 7. Applied load vs. vertical displacement (a) frames 1 and 4, (b) frames 2 and 5, (c) frames 3 and 6.

It may be observed in Figure 7a that the collapse load of frame 4 increases 20.6 % with respect to frame 1, while the displacement decreases 52.5 %. With respect to Figure 7b, it is observed that the collapse load of frame 5 increases 9.52 % with respect to frame 2, and the displacement decreases 43.63 %. It may be observed in Figure 7c that the collapse load of frame 6 increases, representing 14.75 % in percentage with respect to frame 3 and the displacement decreases 45.95 %.

The collapse load increase or vertical displacement decrease is due to the increase of the frame lateral rigidity as a result of the addition of the reinforcing "platen" in the perimeter of the column of the welded joint.
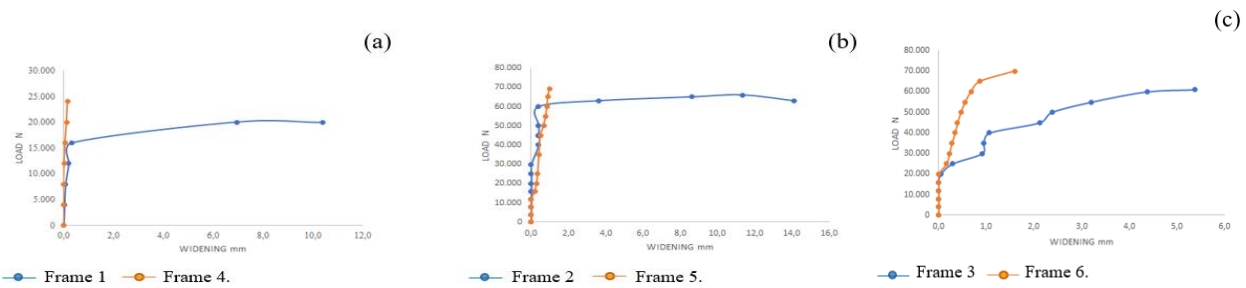
Figure 8. Applied load vs. widening of the cross section of column (C_1), (a) frames 1 and 4, (b) frames 2 and 5, (c) frames 3 and 6.

It is observed in Figure 8 the widening of columns (C_1) in frames 1-4, 2-5 and 3-6. Such widening in frame 4 (Figure 8a) decreases 98.46 % with respect to frame 1. In the case of frames 5 and 2 (Figure 8b) the percentage of decrease represents 92.98 %, while the decrease is 70.20 % with respect to frames 3 and 6 (Figure 8c).

It is observed in Figure 9 the widening of the beam (V_1) of frames 1-4, 2-5 and 3-6. The widening of the beam of frame 4 (Figure 9a) increases 36 % with respect to frame 1. In the case of frames 5 and 2 (Figure 9b) the increase is 2.33 % and for frames 6 and 3 (Figure 9c) the percentage grows to 109.38 %.
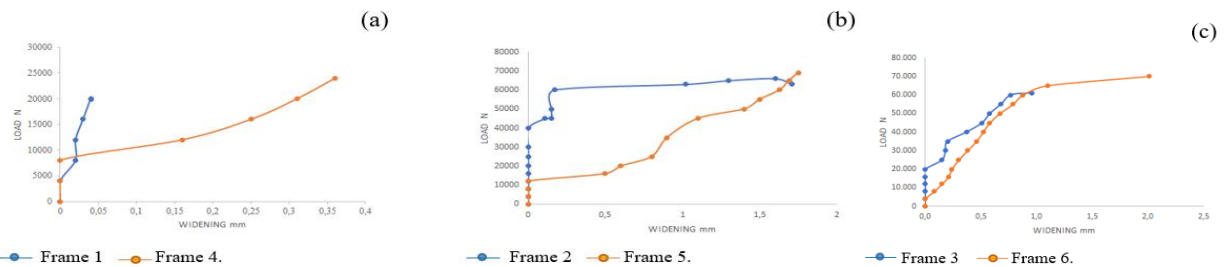
Figure 9. Applied load vs. widening of the cross section of the beam (V_1), (a) frames 1 and 4, (b) frames 2 and 5, (c) frames 3 and 6.
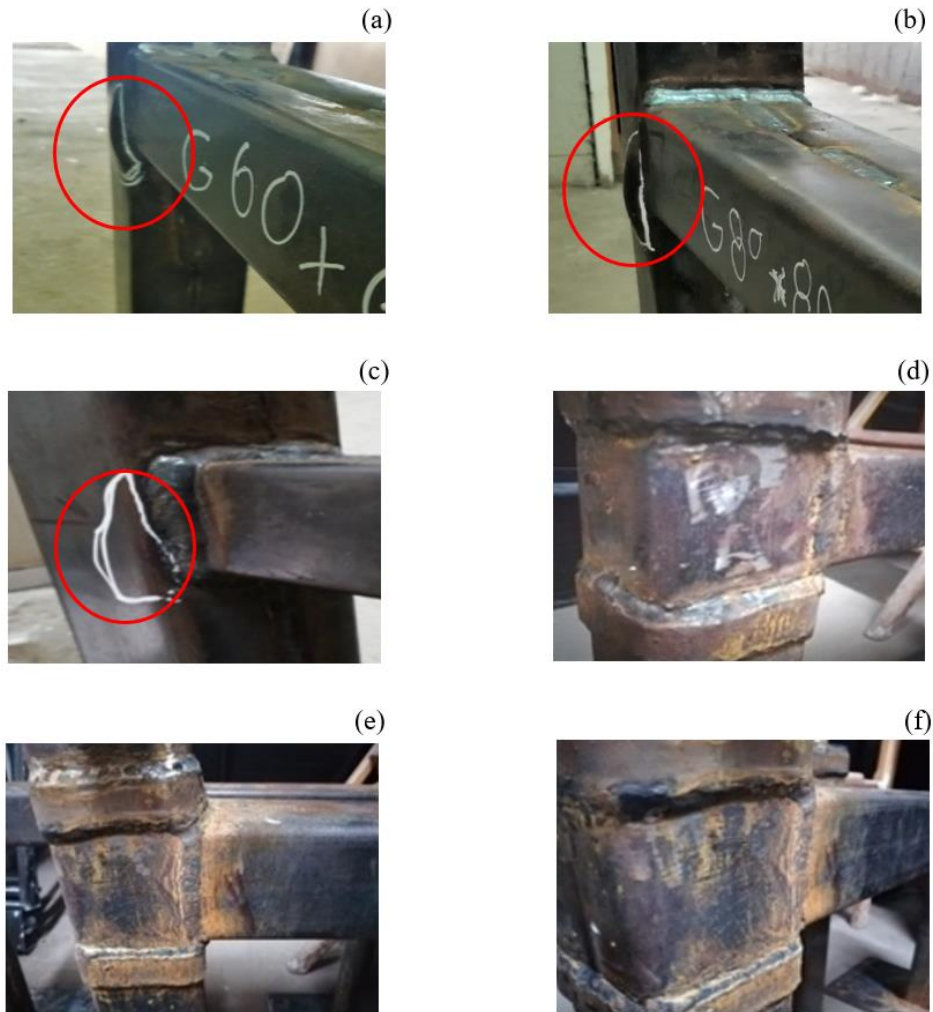
Figure 10. Local buckling distortion of the cross section of the column of the welded joint (a), (b) and (c) frames 1, 2 and 3 (without reinforcement). Distortion of the cross section of the connection beam (d), (e) and (f) frames 4, 5 and 6 (with reinforcement).

Figures 10a, 10b and 10c show the failure (local buckling) (Romero, 2019) that occurs in the column; it is emphasized the distortion of the cross section of the element leading to the formation of the plastic hinge in such element of the welded connection. It is also possible to observe that the reinforcement platens installed in the perimeter of the cross section of the column prevent the failure (local buckling) in the column, thus forming the plastic hinge in the beam of the welded joint (Figures 10d, 10e and 10f), complying with the condition that the beams are plasticized before the columns, and that the energy dissipation mechanism is developed in the beams.

Conclusions

The platens installed in the perimeter of the cross section of the column of the lower connection of frames 4, 5 and 6 prevent the failure (local buckling) and guarantees the formation of the plastic hinge in the beam of the welded joint, thus fulfilling the weak beam – strong column criterion.

The usefulness of the present study is that housings and shopping malls constructed or to be constructed with square tubular profiles might improve their performance by placing reinforcement plates around the column in order to oblige that the beams are plasticized before the columns, that an energy dissipation mechanism is implemented in the beams and that it is prevented the formation of a collapse mechanism.

It has been presented a reinforcement alternative different than the one consulted in the literature, which has produced good results in terms of resistance gain, decrease of displacements, preventing local buckling of columns and guaranteeing the formation of plastic hinges in beams as an energy dissipation mean.

As future work it is recommended to conduct a study of the beam-column connection under cyclic loads, and to observe what is the behavior of the hysteresis loop and its energy dissipation mechanism when using the reinforcement mechanism presented in this work.

References

AISI. (1996). *Cold formed steel design manual.* Washington: American Iron and Steel Institute (AISI).

ASTM A-36. (2014). *Standard specification for carbon structural steel.* West Conshohocken:

American Society for Testing and Materials (ASTM).

Carapaz, D. (2015). *Estudio experimental de columnas tubulares de acero rellenas de hormigón sometidas a carga axial*. Tesis de grado. Quito: Universidad Politécnica Nacional.

Cervera, M. R., Blanco, E. D. (2015). *Resistencia de materiales* 6ta ed. Barcelona: Ediciones UPC.

ANSI/AISC. (2010). *Construcciones de acero, especificación 360-10*. Chicago: American National Standards Institute (ANSI) American Institute of Steel Construction (AISC).

Freddy, D. (2016). *Comportamiento de conexión a momento empernada (viga-columna) entre perfiles tubulares de acero conformados en frio (HSS).* Tesis de grado. Caracas: Universidad Católica Andrés Bello.

Hibbeler, C. (2017). *Mecánica de materiales*. 9na ed. Ciudad de México: Pearson.

Kassimali, A. (2015). *Análisis estructural*. 5ta ed. Ciudad de México: Cengage Learning.

Matthew, F. (2013). *Cyclic bending behavior of hollow structural sections and their application in seismic moment frame systems*. Tesis doctoral. Michigan: University of Michigan.

McCormac, J. (2012). *Diseño de estructuras de acero.* 5ta ed. Ciudad de México: Alfaomega.

NEC-SE-CG. (2014). *Carga no sísmica*. Quito: Norma Ecuatoriana de la Construcción (NEC).

NEC-SE-AC. (2014). *Estructuras de acero*. Quito: Norma Ecuatoriana de la Construcción (NEC).

NEC-SE-DS. (2014). *Peligro sísmico diseño sismo resistente*. Quito: Norma Ecuatoriana de la Construcción (NEC).

Catálogo. (2017). *El acero del futuro*. Quito: Novacero.

Pellicer, D. (2014). *Principio de construcción de estructuras metálicas* 2da ed. Madrid: Bellisco.

Romero, C. (2010). *Comportamiento de conexiones soldadas de tubos estructurales de acero de sección cuadrada sometidos a flexión monotónica*. Tesis de maestría. Maracaibo: Universidad del Zulia.

Romero, C. (2019). Comportamiento elastoplástico de conexiones soldadas en tubos de acero de sección cuadrada sometidos a carga monotónica. *Gaceta Técnica DIC*, 20-(1), 23-29.

Rezaifar, O., Younesi, A. (2017). Analytical study of beam-to-HSS/CFT column connections by trapezoidal external stiffener. *International Journal of Steel Structures,* 17-(2), 1-14.

SAP 2000. (2017). Structural software for analysis and design. Walnut Creek: Computers and Structures, Inc. (CSI).

Seguí, W. (2013). *Steel design* 5th ed. Stanford: Cengage Learning.

Ugarte, A., Sarcos, A., Flores, J. (2006). Comportamiento de tubos cuadrados a flexión monotónica. *Boletín Técnico IMME,* 44-(2), 1-20.

UNIVERSIDAD DEL ZULIA